

Copyright © 1992, by the author(s).
All rights reserved.

Permission to make digital or hard copies of all or part of this work for personal or classroom use is granted without fee provided that copies are not made or distributed for profit or commercial advantage and that copies bear this notice and the full citation on the first page. To copy otherwise, to republish, to post on servers or to redistribute to lists, requires prior specific permission.

**AUTOWAVES FOR IMAGE PROCESSING ON A
TWO-DIMENSIONAL CNN ARRAY OF CHUA'S
CIRCUITS: FLAT AND WRINKLED LABYRINTHS**

by

V. Pérez-Muñuzuri, V. Pérez-Villar, and L. O. Chua

Memorandum No. UCB/ERL M92/75

5 June 1992

COVER PAGE

**AUTOWAVES FOR IMAGE PROCESSING ON A
TWO-DIMENSIONAL CNN ARRAY OF CHUA'S
CIRCUITS: FLAT AND WRINKLED LABYRINTHS**

by

V. Pérez-Muñuzuri, V. Pérez-Villar, and L. O. Chua

Memorandum No. UCB/ERL M92/75

1 June 1992

ELECTRONICS RESEARCH LABORATORY

College of Engineering
University of California, Berkeley
94720

TITLE PAGE

**AUTOWAVES FOR IMAGE PROCESSING ON A
TWO-DIMENSIONAL CNN ARRAY OF CHUA'S
CIRCUITS: FLAT AND WRINKLED LABYRINTHS**

by

V. Pérez-Muñuzuri, V. Pérez-Villar, and L. O. Chua

Memorandum No. UCB/ERL M92/75

1 June 1992

ELECTRONICS RESEARCH LABORATORY

College of Engineering
University of California, Berkeley
94720

AUTOWAVES FOR IMAGE PROCESSING ON A TWO-DIMENSIONAL CNN ARRAY OF
CHUA'S CIRCUITS: FLAT AND WRINKLED LABYRINTHS

V. Pérez-Muñuzuri, V. Pérez-Villar

*Dept. Física de la Materia Condensada
Facultad de Físicas
15706 University of Santiago de Compostela. Spain.*

and L.O. Chua

*Dept. of Electrical Engineering and Computer Sciences
University of California, Berkeley, CA 94720. USA.*

June 1992

Abstract

We describe a two-dimensional CNN array of resistively coupled Chua's circuits that deal with some elementary aspects of spatial cognition, namely; recognizing open curves and objects from closed ones and locating the shortest path between two locations. In this case, two situations are analyzed: flat and wrinkled surfaces. The performance of this model was examined using computer simulations although this method can be implemented electronically via VLSI technology.

This work is supported in part by the Office of Naval Research under grant N00014-89-J-1402 and the National Science Foundation grant MIP-8912639.

1. Introduction

Biological systems ordinarily perform reasoning and logical decisions beyond the capabilities of our most sophisticated computer systems. Intuitively, these tasks seem to require mechanisms in which each aspect of the information in the situation can act on other aspects, simultaneously influencing and being influenced by them. To implement these mechanisms a class of models called "*Parallel Distributed Processing (PDP)*" have been developed [1]. These models assume that information processing takes place through the interactions of a large number of simple processing elements called units, each sending excitatory and inhibitory signals to other units.

PDP models are related to "*analog neural networks*". Their key features are asynchronous parallel processing, continuous-time dynamics and global interactions of network elements. In the Hopfield networks [2,3] each neuron is coupled with every other and the corresponding integrated circuit is not technologically feasible.

Cellular Neural Networks (CNN) [4,5] have been developed to overcome these problems. They possess the key features of neural networks, but each unit/cell of the CNN is connected only to its neighbor cells. Each cell contains linear and nonlinear circuit elements. Cells not directly connected together may affect each other indirectly because of the propagation effects of the continuous-time dynamics of the CNN. The CNN can perform parallel signal processing in real time, many examples of its possibilities can be found in the literature [6]; e.g. noise removal, corner extraction, edge extraction, connectivity analysis, the Radon transform, thinning and half-toning, to mention only the most relevant.

Recently, Krinsky et al. [7,8] have proposed what they called "*The Autowave Principles for Parallel Image Processing*". Autowaves represent a particular class of

nonlinear waves, which spread in active excitable media at the expense of the energy stored in the medium. Under some conditions, these waves can be represented essentially by two states, one is assigned to those parts of the system that are moving along a limit cycle, while the remaining points are represented by the second state.

The fundamental properties of autowaves differ basically from those of classical waves in conservative systems. Thus, autowaves do not reflect or interfere, but annihilate and diffract. Using these properties, Krinsky et al. prove the ability of the autowaves for some image processing operations, such as contrast regulation, restoration of a broken contour, and edge detection [7]. Principles of parallel analog information processing by means of distributed systems are also discussed in Ref. [9].

By coupling several Chua's circuits we have been able to show, analytically the existence of traveling wave solutions in this system [10,11]. Traveling waves are a particular case of autowaves since they only trigger from one stable equilibrium state to a second one where they remain from then on. The diffraction and annihilation of these waves are found to be extremely interesting properties for image analysis. The purpose of this paper is to show that a two-dimensional CNN array of coupled Chua's circuits can be used for image processing. We will bring to focus some examples, namely; distinction between closed and open curves and finding the shortest path in a labyrinth.

In the last case, two possibilities can appear in real life, since the labyrinth can be flat or wrinkled. For example, the first situation is typical for hospitals or large office buildings where large open surfaces with only walls or furniture to block the way are common. The second situation could correspond to the case of anyone going from point A to point B separated by some hills with gentle and steep slopes.

In this case, the shortest path may not be the one that takes less time since other factors must be considered; for example, the available stored energy. In other words, instead of taking the geometrically shortest path between A and B, that may include climbing steep hills, it may be better to go around the obstacle in order to save energy.

Due to the fact that our array is a set of resistively coupled Chua's circuits, it has been found that the velocity of the traveling waves decreases with the diffusion coefficient and can fail to propagate at, or below, some critical value of the diffusion coefficient. This effect can only be found in a discrete model where the internal dynamics of each circuit cell plays an important role and it can potentially be used to solve three-dimensional spatial image problems with a two-dimensional non-homogeneous array of Chua's circuits.

2. Model of the Two-Dimensional CNN Array of Chua's Circuits

The basic unit (cell) of our two-dimensional CNN array is a Chua's circuit [12-17] (Fig.1), a simple active nonlinear circuit which exhibits a variety of bifurcation and chaotic phenomena. The circuit contains three linear energy-storage elements (an inductor and two capacitors), a negative linear conductance, and a single nonlinear positive resistor. Every cell is coupled with their four closest adjacent neighbors through linear resistors, thereby simulating a diffusion process.

The circuit dynamics for each cell can be described by a third-order autonomous nonlinear differential equation. In particular, we will choose the dimensionless form given by (1.1) in Ref. [12], which we rewrite for each circuit cell at the position (i,j) of the array as,

$$\begin{aligned}
\dot{x}_{i,j} &= \alpha (y_{i,j} - h(x_{i,j})) + D [x_{i-1,j} + x_{i+1,j} + x_{i,j-1} + x_{i,j+1} - 4 x_{i,j}] \\
\dot{y}_{i,j} &= x_{i,j} - y_{i,j} + z_{i,j} \\
\dot{z}_{i,j} &= -\beta y_{i,j}
\end{aligned} \tag{1}$$

where $1 \leq \{i,j\} \leq n$, n is the size of the array. $h(x)$ describes the three- segment piecewise- linear curve of the nonlinear resistor described by

$$\begin{aligned}
h(x) &= m_1 x + (m_0 - m_1) x_2 + \varepsilon & x \geq x_2 \\
&= m_0 x + \varepsilon & x_1 \leq x \leq x_2 \\
&= m_1 x + (m_0 - m_1) x_1 + \varepsilon & x \leq x_1
\end{aligned} \tag{2}$$

where ε is a small constant called the "DC offset".

We will choose $x_1 = -1$ and $x_2 = 1$. Observe that in view of the symmetric configuration of the nonlinear characteristics (i.e. its integral is equal to zero), it is necessary to include an offset, $\varepsilon \neq 0$, in order to have a traveling wave solution [10].

In Eq. (1), D represents the diffusion coefficient of the variable x , and is given by $\alpha/(G R)$ in its dimensionless form¹, where G is the conductance in Siemens of the linear resistor in the Chua's circuit, and R is the coupling resistance in Ohms. D is assumed to be constant in the first two cases presented in this paper. However, a diffusion coefficient which is a function of the position, $D = D(i,j)$, is necessary to describe a wrinkled labyrinth, as we will show later.

The set of fixed parameters used throughout this paper is $\{\alpha, \beta, m_0, m_1\} = \{9, 30, -1/7, 2/7\}$, $G = 0.7$ and $\varepsilon = -1/14$. For these values of the parameters the

¹We use the same scaled parameters as in Ref. [17].

propagation failure mentioned above occurs at, or below, some critical value of the diffusion coefficient $D^* = 0.51$ ($R^* = 25$).

The equilibrium states of Eq. (1) obtained by setting $\dot{x}_{1,j} = \dot{y}_{1,j} = \dot{z}_{1,j} = 0$ are summarized as follows,

State	x	y	z
P_+	$(m_1 - m_0)/m_1 - \epsilon/m_1$	0	$(m_0 - m_1)/m_1 + \epsilon/m_1$
P_0	$-\epsilon/m_0$	0	ϵ/m_0
P_-	$(m_0 - m_1)/m_1 - \epsilon/m_1$	0	$(m_1 - m_0)/m_1 + \epsilon/m_1$

Here x , y and z are vectors of dimension $n \times 2$. Each of these three equilibrium states represents a solution to Eq. (1) for all values of the parameters.

The nonlinear boundary value problem described by equations (1) and (2) was completed by imposing zero-flux boundary conditions. A uniform time step of 0.01 was used throughout as the differential equations were integrated using the explicit Euler method. The spatial step size is kept at a constant value equal to one, as a consequence of our assumption of a discrete array.

3. Examples of Homogeneous Two-Dimensional CNN Array of Chua's Circuits for Image Processing

Here we present two examples for illustrating the possibilities of using a two-dimensional CNN array of Chua's circuits for image processing. Recall that autowaves, and by definition, traveling waves, are not reflected by obstacles and boundaries and do not interfere when two of them collided with each other. Our model is able to recognize open curves and shapes from closed ones, and can identify the shortest path between two locations. Since the autowaves propagate throughout the

medium with a constant velocity, a large number of circuits operate simultaneously. On the other hand, classical methods for detecting closed curves usually consists of scanning all possible points of the array in order to locate first the objective being classified, and then following the boundary of the object, by trial and error, until the closed curve is identified.

The problem for finding the shortest path between two points is equivalent to solving the *traveling salesman problem* [3,18,19]. In this frequently studied optimization problem, a salesman is required to visit in some sequence each of n cities; the problem is to determine the shortest closed tour in which every city is visited only once. A Hopfield neural network can solve this problem by defining a specific synaptic connection between neurons that minimizes an energy function [3]. The main difference between the classical solution of the *traveling salesman problem* and our approach is the connection between neurons. In the first case, the neurons are connected between them in a specific way in order to solve a specific problem, while in our model each cell is only connected with the nearest neighbors.

For the two examples to be presented below, we make the following assumptions:

(1) The input image for pattern cognition is "*stored into the memory*" of our array by keeping (i.e. clamping) those circuit cells that coincide with the position of the obstacles, at the same initial state, at all times. This assumption is equivalent, from the point of view of numerical simulation, to imposing some kind of boundary conditions for the obstacles so that traveling waves can surround them because of the diffraction properties of the autowaves.

(2) Only binary images are assumed in these two examples. The two allowed

states coincide with the two equilibrium states P_+ and P_- in Chua's circuits.

(3) A traveling wave is always initiated at the left top corner of our array by setting one of the Chua's circuits at the positive equilibrium state P_+ while maintaining the remaining cells at P_- . The traveling wave triggers from P_- to P_+ at constant velocity, and spreading throughout the image. We should point out that even though each cell can settle to either P_{\pm} , the state dynamics of each node are continuous (the state of a node is not binary valued).

The pictures presented in this section are obtained by computer simulations with a SUN 4 Workstation. The numerical simulations take 15 minutes to "complete" an array of 45 x 45 Chua's circuits.

3.1. Detection of Closed Curves

Figure 2.a shows two possible obstacles that our model can detect and differentiate. One of them is an open cavity (left top of the figure) while the second one is a closed obstacle.

The set of computer snapshots in Fig. 2 shows the traveling wave propagating throughout the input image. Because of the dispersion but not interference and reflection properties of autowaves, the traveling wave surrounds the wall of the open cavity and differentiates the closed obstacle by bypassing it, from those that are opened by filling up the open space. Thus, the closed objects will remain at the initial state P_- . This criterion can distinguish a closed curve from an unclosed one.

This method can be implemented by adding a simple decision circuit designed to

identify the cells that have triggered from a negative initial state to a positive final state. Another possibility is to generate the difference picture of the result of this transformation from the original image. Then, the closed curves can be detected. Observe that unlike many other approaches, this method for closedness detection is invariant against translations, rotations and scaling.

This application of autowaves for image processing can also be implemented by a CNN cloning template [20].

3.2. Shortest Path in a Labyrinth

This application follows from the first example. After a traveling wave is initiated at the left top corner of Fig.3a, it propagates throughout the image (see consecutive snapshots 3b to 3f). Because of its constant velocity, the shortest path will coincide with the path that takes the least time. Let us suppose that our wave must find which is the shortest path to reach the left bottom corner of the image. In this case, our autowave "*explores*" all the possible ways to reach that point. In the successive snapshots shown in figure 3, observe that upon hitting the obstacle, centered at cell (30,10), the traveling wave splits and eventually surrounds this object (Fig. 3d), and finally annihilates each other when the two wave fronts collided with each other [7].

Figure 3f shows the final state when the program stops after the wave reaches the left bottom corner. With the help of a simple external circuit, the times at which the cells had triggered from state P_- to P_+ can be stored and compared in order to determine the path that takes the least time to reach the final destination.

4. The Wrinkled Labyrinth

In this case, a new third degree of freedom is added to our problem. Suppose the ground is not flat but wrinkled. In this case, the shortest path is the path that takes the least energy. This class of problems could be useful for moving systems with a limited amount of stored energy between two points on an undulated surface.

From a numerical point of view, this situation can be achieved with a discretized array of cells, each one connected with their adjacent neighbors through different linear resistors R . These resistors, which vary from R_{\min} to R_{\max} , are used to code the difficulty of slopes. Gentle slopes will correspond to values of R which are close to R_{\min} , while steep slopes to values of R close to R_{\max} .

Then, the input image is a black and white photo with different tonalities of greys of the wrinkled terrain where for example, the clearest parts of the photo correspond to the higher zones of the terrain and are therefore identified with R_{\max} . The remaining tonalities are identified with corresponding values of resistors until the minimum allowed value, R_{\min} , is reached. This can be achieved experimentally by fixing the value of the coupling linear resistors with voltage- controlled impedances [21,22]. Thus, the different grey tonalities are discretized in discrete voltages levels.

As mention in the Introduction, the discretized version of the coupled Chua's circuits exhibits an interesting effect usually found in nerve propagation, namely; "*Propagation Failure*". By choosing those points of the terrain that are unreachable for our autowave to values of R at, or greater than some critical value R^* where the "*failure*" phenomenon appears, the traveling wave propagating throughout the array will fail to propagate from those points that remain isolated from the rest of the

image.

Figure 4a represents a possible undulated terrain. This image shows the discretized values of the resistance for the interval, $1 < R < 30$. The cell located near the top of the *Mexican hat* have been assumed to be unreachable for the autowave and hence, their coupling resistances have been set to values of $R \geq R^* = 25$. The objective is to find the best path between the top cell (1,1) and the bottom corner at cell (45,45) of Fig.4a. As in the preceding examples, the image processing begins when a traveling wave is initiated at the top cell (1,1) of Fig.4a by setting the cell (1,1) at the steady state P_+ at $t = 0$, while the remaining cells are set at P_- . After that ($t > 0$), the autowave spreads throughout the wrinkled labyrinth, as expected.

Obviously, for the homogeneous case, the shortest path is along the diagonal of the array. In this case, in view of the inaccessibility of the top of the Mexican hat, the autowave finds the best path by flowing and engulfing around the obstacle. The set of figures 4b to 4f shows this behavior. In those zones of the array where the coupling resistance is close to the critical value R^* , the autowave velocity decreases, while in the other favorable zones (gentle slopes) its velocity increases. Once the autowave reaches our destination cell (45,45) at the bottom corner; it stops to propagate (Fig.4f).

This approach allows us to save the system's stored energy by choosing the most favored path; i.e. the path where the diffusion processes involved in the wave propagation are favored.

5. Conclusions

We have shown that a two-dimensional CNN array of Chua's circuits can be used for image analysis. Results similar to those proposed by Krinsky et al. [7] for autowave propagation have been reproduced numerically, namely; detection of closed curves and finding the shortest path in a labyrinth.

Those results were obtained in a resistively coupled homogeneous array of Chua's circuits when a traveling wave propagates throughout an input image. Obviously, the examples shown in section 3 are a special case of the wrinkled labyrinth. By using a non-homogeneous array it is possible to analyze three-dimensional surfaces, or undulated surfaces, in order to find the best path (i.e. the one that favors the autowave propagation) between two points. The unreachable places for our autowave can be fixed by setting the corresponding cells of the CNN array to be coupled with their neighbors through resistances at, or greater, values than R^* . Since for $R > R^*$ the wave fails to propagate [10,11], these points of the input image will remain isolated from the rest, as if they are obstacles.

It is important to remark that for autowave processes the traveling wave velocity scales as $(R^* - R)^{1/2}$, i.e. for values of the resistance lower than R^* and close to the allowed R_{\min} the changes in the values of the velocity are small if we compare with R . Consequently, for the wrinkled labyrinth shown in figure 4a, our autowave can not identify perfectly that the best path is to go through the lower values of the resistance in Fig.4a. To solve this problem the input image can be discretized for values of the resistance closer to R^* . In this case, the ability of the autowave to identify the best path is improved, but the process becomes slower.

The wrinkled labyrinth is a powerful technique to discriminate steep slopes

from gentle slopes, as well as to indicate to an autonomous system in real time which places are unreachable, depending on its stored energy. This technique is based on the observation that the state of each cell can be changed in order to vary the value of the critical resistance R^* via some external controlling parameters [11].

The possibility of building large arrays of Chua's circuits via VLSI technology, as well as the use of voltage-controlled resistors to store the undulated surfaces, make this autowave approach a unique tool for real time image processing.

Acknowledgements: We want to thank Drs. J.L. Porteiro and Tibor Kozek for helpful discussions.

REFERENCES

- [1] J.L. McClelland and D.E. Rumelhart. *"Parallel distributed processing"*. MIT Press, 1988.
- [2] J.J. Hopfield. *"Neural networks and physical systems with emergent computational abilities"*. Proc. Natl. Acad. Sci. USA. 79 (1982) 2554-2558, and, *"Neurons with graded response have collective computational properties like those two-state neurons"*. Proc. Natl. Acad. Sci. USA. 81 (1984) 3088-3092.
- [3] J.J. Hopfield and D.W. Tank. *"Computing with neural circuits: a model"*. Science. 233 (1986) 625-633.
- [4] L.O. Chua and L. Yang. *"Cellular Neural Networks: Theory"*. IEEE Trans. Circuits and Systems. 35 (1988) 1257-1272.
- [5] L.O. Chua and L. Yang. *"Cellular Neural Networks: Applications"*. IEEE Trans. Circuits and Systems. 35 (1988) 1273-1290.
- [6] L.O. Chua, L. Yang and K.R. Krieg. *"Signal processing using Cellular Neural Networks"*. Journal of VLSI Signal Processing. 3 (1991) 25-51.
- [7] V.I. Krinsky, V.N. Biktashev and I.R. Efimov. *"Autowaves principles for parallel image processing"*. Physica 49D (1991) 247-253.
- [8] L. Kunhert, K.I. Agladze and V.I. Krinsky. *"Image processing using light-sensitive chemical waves"*. Nature 337 (1989) 244-247.
- [9] A.S. Mikhailov. *"Engineering of dynamical systems for pattern recognition and information processing"* in Nonlinear Waves 2. A.V. Gaponov-Grekhov, M.I. Rabinovich and J. Engelbrecht, Eds. Springer-Verlag (1989). pp. 104-115.
- [10] V. Pérez-Muñuzuri, V. Pérez-Villar and L.O. Chua. *"Traveling wave front and its failure in a one-dimensional array of Chua's circuits"*. To appear at J. Circuits Sys. Comp. (March 1993).

- [11] V. Pérez-Muñuzuri, V. Pérez-Villar and L.O. Chua. "Propagation failure in linear arrays of Chua's circuits". International. J. of Bif. and Chaos. 2 (June 1992).
- [12] L.O. Chua, M. Komuro and T. Matsumoto. "The double scroll family, parts I and II". IEEE Trans. Circuits Sys. CAS-33 (1986) 1073-1118.
- [13] J. Cruz and L.O. Chua. "A CMOS IC nonlinear resistor for Chua's circuit" Submitted IEEE Trans. Circuits Sys. (1992).
- [14] L.O. Chua and G.N. Lin. "Canonical realization of Chua's circuit family". IEEE Trans. Circuits Sys. CAS-37 (1990) 885-902.
- [15] M.P. Kennedy. "Robust Op amp realization of Chua's circuit". Frequenz. 46 (3-4) (1992).
- [16] T. Matsumoto. "A chaotic attractor from Chua's circuit". IEEE Trans. Circuits Syst. CAS-31 (1984) 1055-1058.
- [17] T. Matsumoto, L.O. Chua and M. Komuro. "The double scroll". IEEE Trans. Circuits Syst. CAS-32 (1985) 797-81.
- [18] J.J. Hopfield and D.W. Tank. Biol. Cibern. 52 (1985) 141.
- [19] M.R. Garey and D.S. Johnson, "Computers and Intractability". Freeman, New York (1979).
- [20] T. Matsumoto, L.O. Chua and R. Furukawa. "CNN cloning template: hole-filler". IEEE Trans. Circuits Syst. 37 (1990) 635-638.
- [21] R. Senani and D.R. Bhaskar. "Realization of voltage- controlled impedances". IEEE Trans. Circuits and Syst. 38 (1991) 1081-1086.
- [22] K.W. Nay and A. Budak. "A voltage- controlled- resistance with wide dynamic range and low distortion". IEEE Trans. Circuits and Syst. 30 (1983) 770-772.

FIGURE CAPTIONS

Figure 1: Chua's circuit consists of a linear inductor L , a linear resistor of conductance G , two linear capacitors C_1 and C_2 , and a nonlinear resistor known as the Chua's diode. Each unit is connected to its neighbors through linear resistors R at node V_1 .

Figure 2: (a) The input image; a cavity and an obstacle on a 45×45 CNN array of Chua's circuits. From (b) to (f) the traveling wave initiated at the top left cell (1,1) of the figure spreads throughout the image surrounding the obstacles and entering the cavity. In this way, both objects are identified.

Figure 3: (a) The input image; a labyrinth defined by three obstacles on a two-dimensional array of Chua's circuits. From (b) to (f) the traveling wave initiated at the top left cell (1,1) of the input image spreads throughout the image. The autowave properties of annihilation and diffraction are clearly seen. The traveling wave stops when it reaches the final cell (45,45), left bottom of the figure.

Figure 4: The wrinkled labyrinth. (a) The input image; a Mexican hat. This image shows the discretized values of the resistance in the interval, $1 < R < 30$. From (b) to (f) the traveling wave initiated at the top of the figure (a) spreads throughout the image. Picture (f) shows the final state when the autowave reaches its destination. The hole at the center of the picture represents those places that are unreachable for the autowave.

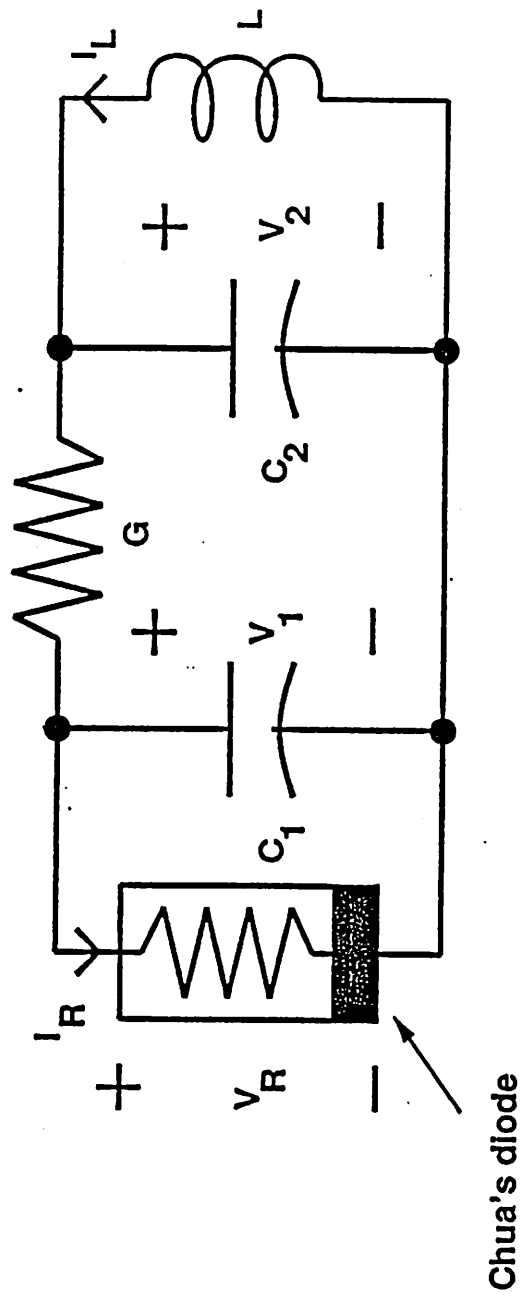
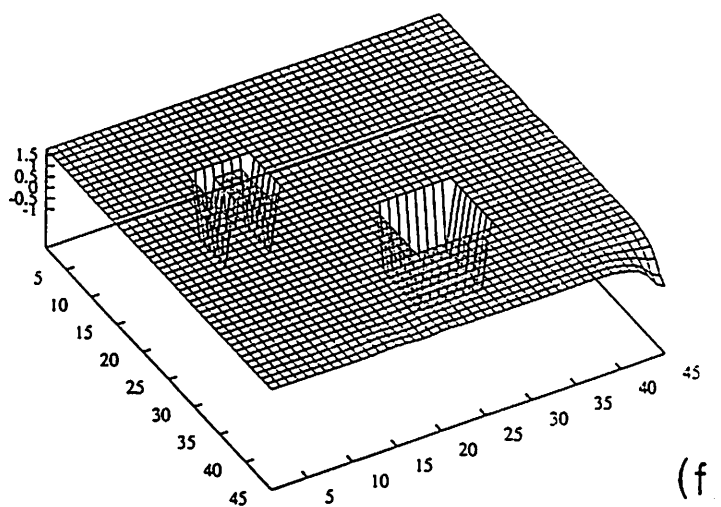
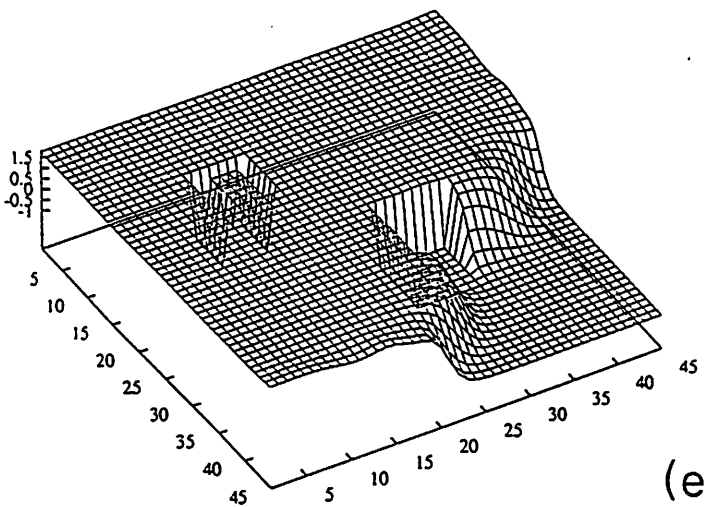
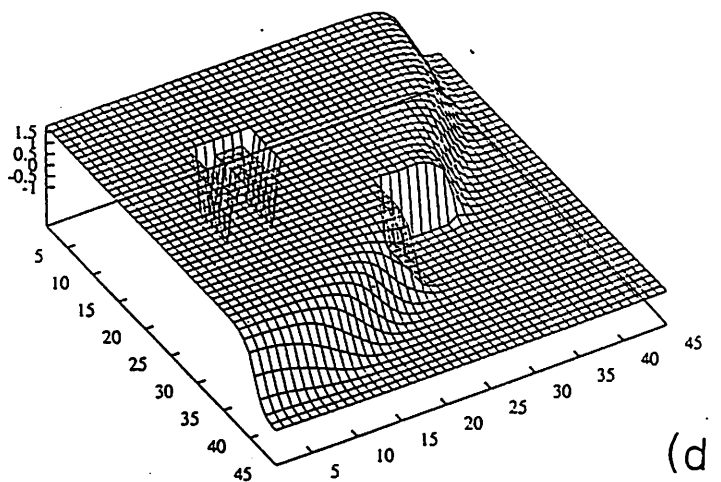
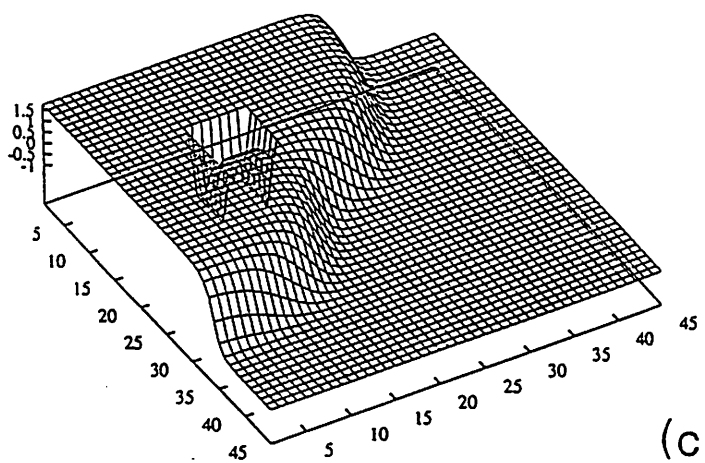
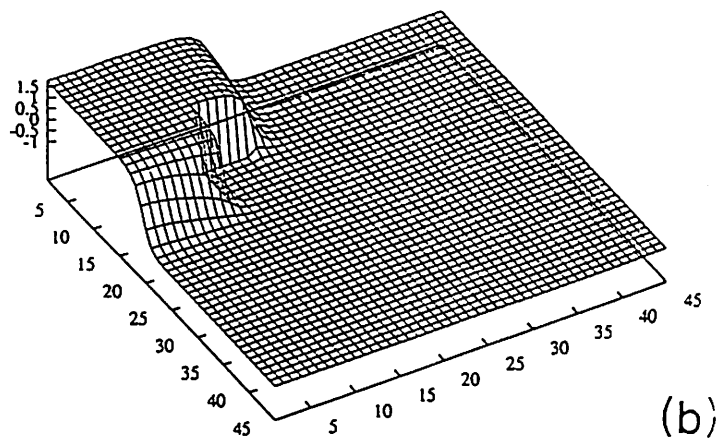
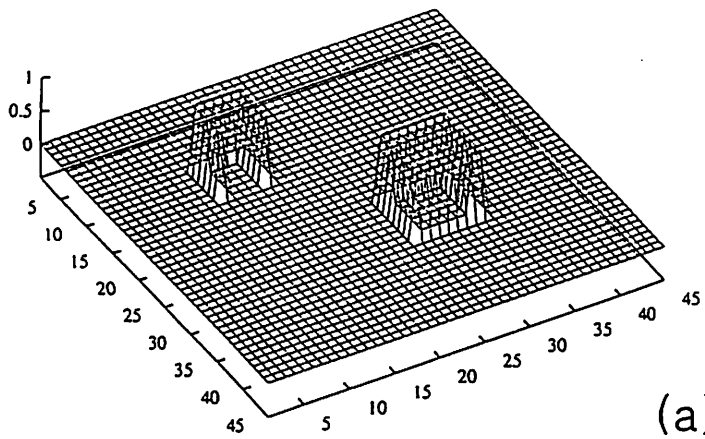
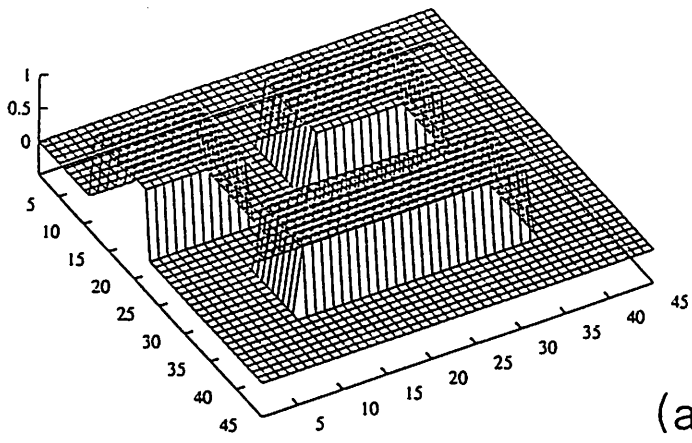
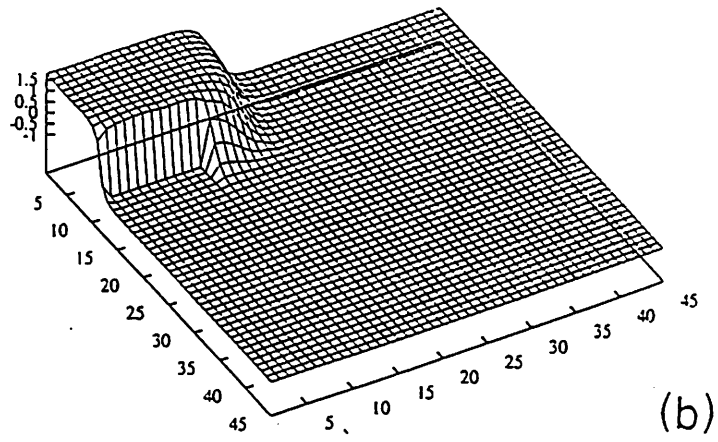


Figure 1

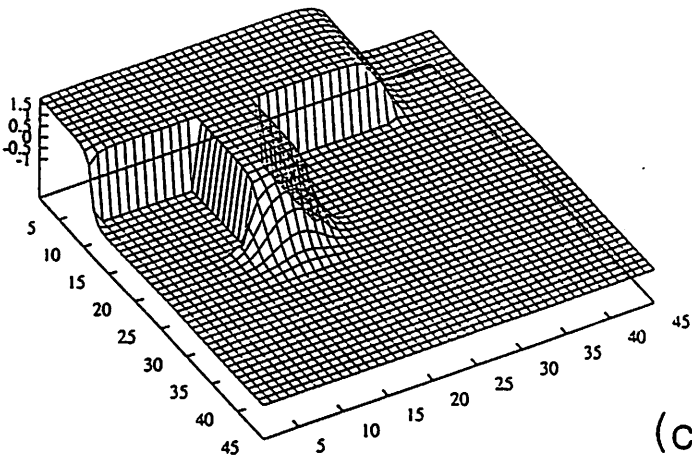




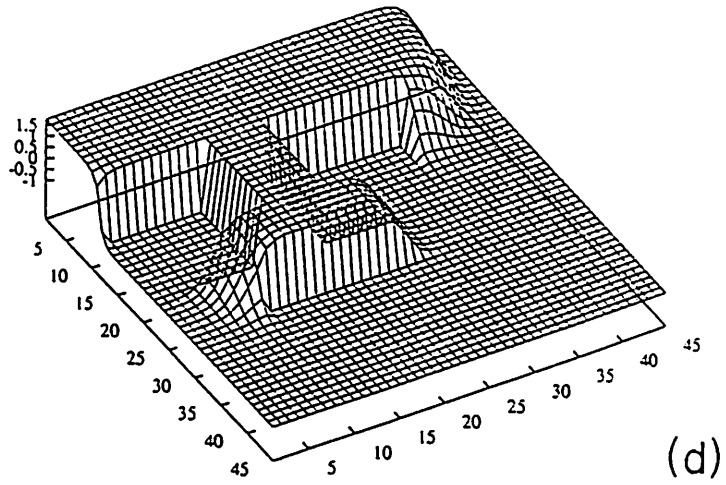
(a)



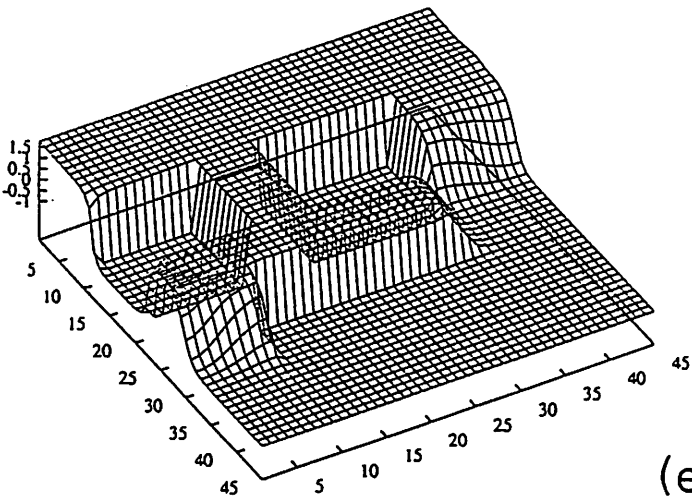
(b)



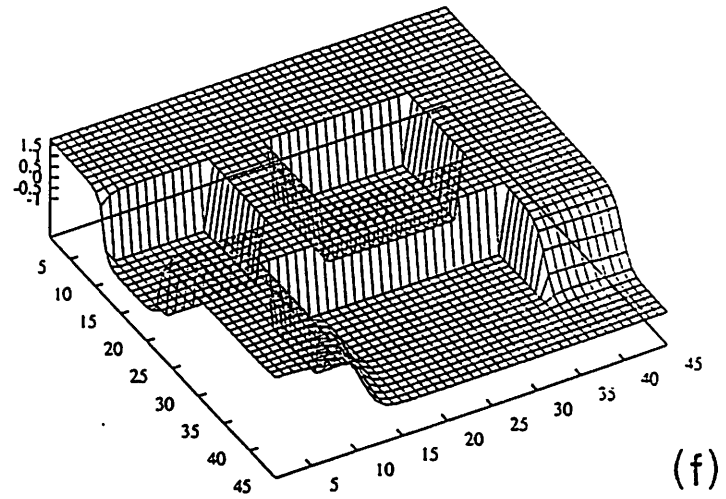
(c)



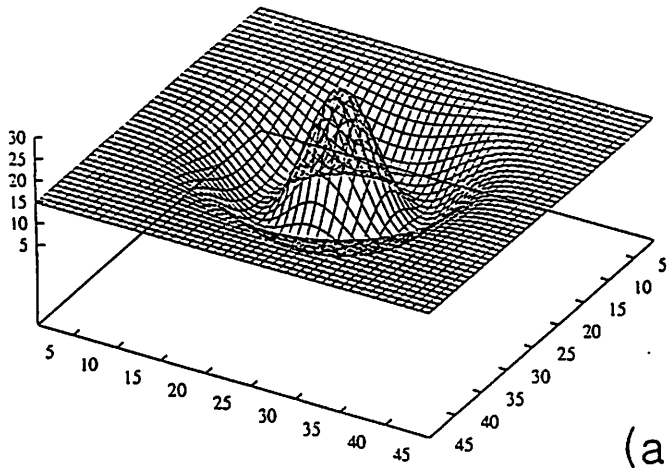
(d)



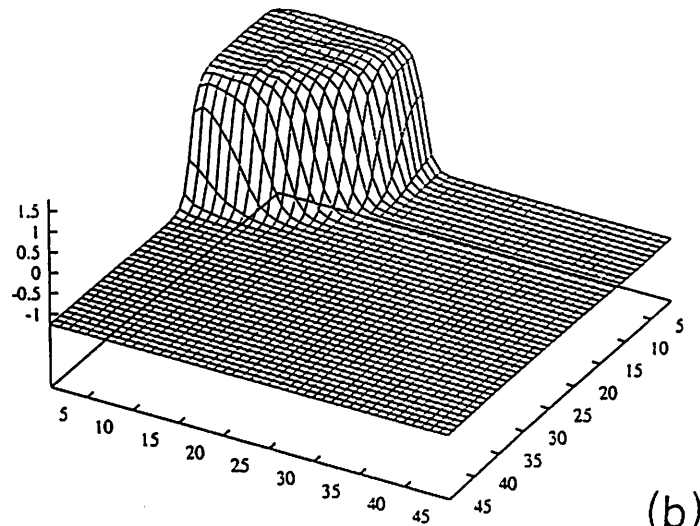
(e)



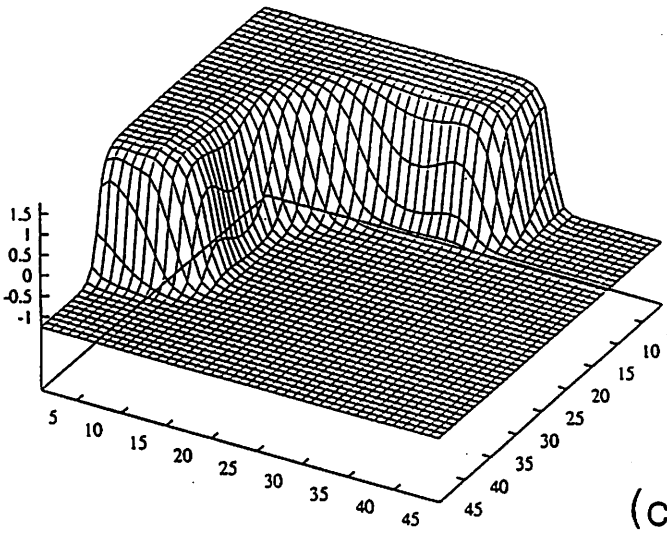
(f)



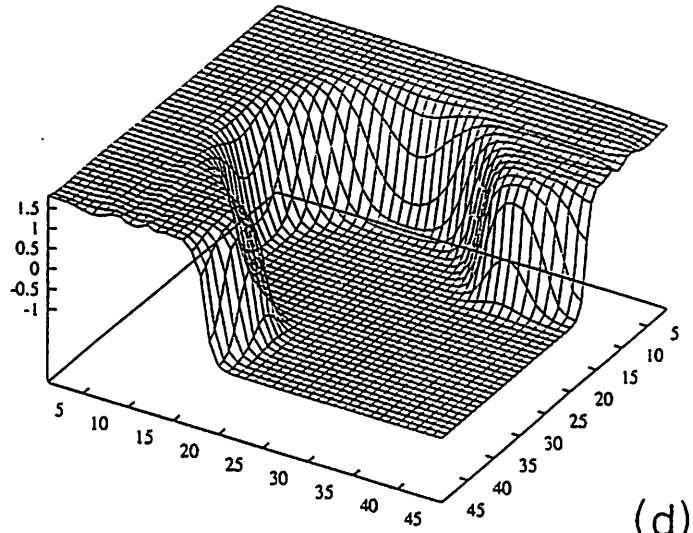
(a)



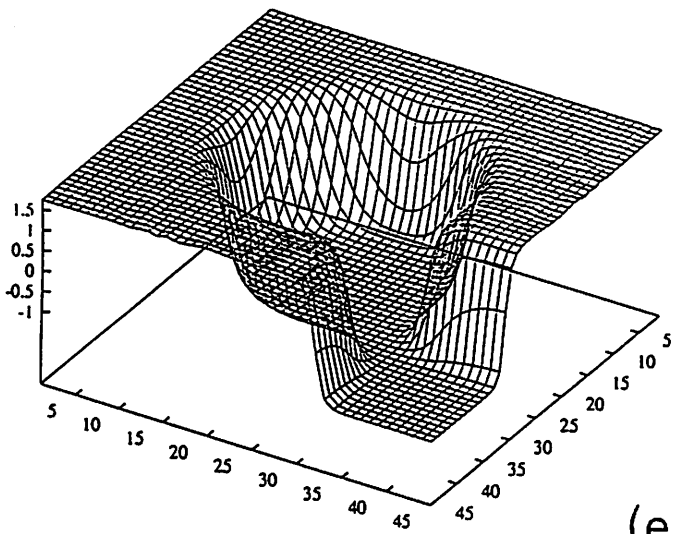
(b)



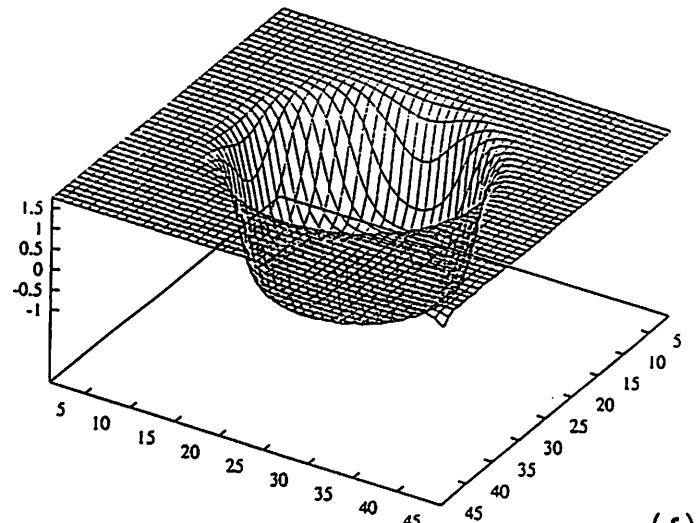
(c)



(d)



(e)



(f)